B_2N_2-Dibenzo[*a,e*]pentalenes: Effect of the BN Orientation Pattern on Antiaromaticity and Optoelectronic Properties

Journal:	*Journal of the American Chemical Society*
Manuscript ID:	ja-2015-050562.R1
Manuscript Type:	Communication
Date Submitted by the Author:	05-Jun-2015
Complete List of Authors:	Wang, Xiao-Ye; Max Planck Institute for Polymer Research, Narita, Akimitsu; Max Planck Institute for Polymer Research, Feng, Xinliang; Dresden University of Technology, Müllen, Klaus; Max Planck Institute for Polymer Research,

B_2N_2-Dibenzo[*a,e*]pentalenes: Effect of the BN Orientation Pattern on Antiaromaticity and Optoelectronic Properties

Xiao-Ye Wang,[†] Akimitsu Narita,[†] Xinliang Feng,*[,‡] Klaus Müllen*[,†]

[†] Max Planck Institute for Polymer Research, Ackermannweg 10, 55128 Mainz, Germany

[‡] Center for Advancing Electronics Dresden (cfaed) & Department of Chemistry and Food Chemistry, Technische Universität Dresden, 01062 Dresden, Germany

Supporting Information Placeholder

ABSTRACT: Two BN units were embedded in dibenzo[*a,e*]pentalene with different orientation patterns, which significantly modulated its antiaromaticity and optoelectronic properties. Importantly, the vital role of BN orientation in conjugated molecules with more than one BN unit was demonstrated for the first time. This work indicates a large potential of the BN/CC isosterism for the development of new antiaromatic systems and highlights the importance of precise control of the BN substitution patterns in conjugated materials.

Aromaticity is one of the most important concepts in chemistry. Over decades, aromatic compounds have always been the majority of organic conjugated molecules, whereas antiaromatic ones, which exhibit completely different properties, have been relatively underexplored.[1] Recently, the fundamental interest in BN-substituted benzene, in which a C=C bond is replaced with its isoelectronic B–N bond, has triggered growing research efforts in azaborine chemistry.[2] The BN/CC isosterism not only expands the structural diversity of organic compounds and enriches the fundamental understanding of aromaticity,[3] but also provides promising materials for various applications, for example, in hydrogen storage,[4] biomedicine,[5] and organic electronics.[6] A number of BN-substituted aromatic systems have already been reported, including BN-substituted benzene,[7] naphthalene,[8] indole,[9] phenanthrene,[10] anthracene,[11] triphenylene,[12] pyrene,[13] coronene,[14] and other polycyclic aromatic compounds.[15] However, the application of this BN substitution strategy in antiaromatic systems has been extremely limited.[2] On the other hand, in conjugated systems incorporating more than one BN unit, there is a fundamental question about the effect of the BN orientation patterns on their chemical and physical properties. Nevertheless, to the best of our knowledge, there has been no investigation on this topic up to now, presumably due to the great challenge of precisely manipulating the BN orientation in the same conjugated skeleton.

Dibenzo[*a,e*]pentalene (**DBP**) is a ladder-type polycyclic hydrocarbon which possesses an antiaromatic character with a $4n\pi$-electron periphery.[16] Since the first synthesis in 1912, **DBP**s have attracted considerable research interest regarding the development of convenient synthetic methods and the exploration of their applications in materials science.[17] Herein, we chose the **DBP** skeleton to investigate the effect of BN substitution on the properties of such antiaromatic systems.[18] We synthesized two B_2N_2-incorporated **DBP**s with different orientation patterns of BN units (Chart 1, *anti*-orientation: termed as **BNNB-DBP**; *syn*-orientation: termed as **BNBN-DBP**). X-ray single-crystal analysis revealed their planar structures, and theoretical, spectroscopic, and electrochemical studies demonstrated that the antiaromaticity and optoelectronic properties have been significantly modulated by the different BN substitution patterns.

Chart 1. DBP and its BN-substituted derivatives.

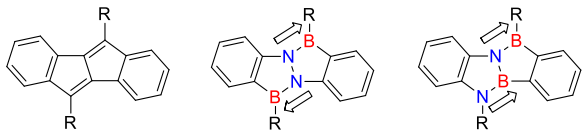

The synthetic routes to **BNNB-DBP** and **BNBN-DBP** are illustrated in Scheme 1. First, 1-bromo-2-nitrobenzene (**1**) was converted to 2,2'-dibromohydrazobenzene (**2**) under a reductive condition. Then *t*-BuLi was used to perform deprotonations and lithium-halogen exchanges simultaneously at 0 °C to generate a tetralithiated intermediate, which was subsequently reacted with dimethoxy mesitylborane to obtain **BNNB-DBP** in 68% yield in one pot. Compared to the electrophilic borylation method used by Cui *et al*.,[18] this approach is not affected by the electron density of the reactants and can also avoid high reaction temperatures, which make it applicable to a broader scope of substrates. The target compound was stable enough to be purified by column chromatography on silica gel and recrystallization from CH_2Cl_2/hexane to give colorless crystals. However, when dimethoxy phenylborane was used in the final step, only a complex mixture was obtained, indicating the necessity of bulky protecting groups on the boron centers in this nucleophilic substitution step.

The skeleton of the other isomer **BNBN-DBP** was constructed in a stepwise manner (Scheme 1). First, *N*-mesityl-benzene-1,2-diamine (**3**) was condensed with (2-bromophenyl)boronic acid in refluxing *o*-xylene to afford precursor **4** in 56% yield. Then lithiation of **4** was performed with *t*-BuLi at –78 °C to avoid decomposition of the diazaboroline ring. Subsequent nucleophilic substitution reactions of the dilithiated species with dimethoxy mesitylborane afforded **BNBN-DBP** in 70 % yield. The solvents played an important role in this step, probably due to the different solubility of LiOMe which was generated after the ring closure. When

THF was first used, **BNBN-DBP** could not be obtained, presumably due to the ring opening of the product, which was caused by the nucleophilic attack of the solubilized LiOMe at the unprotected boron, namely the one not connected to the mesityl group (Scheme S1). Nevertheless, by using diethyl ether or dibutyl ether as the solvent, LiOMe could be mostly precipitated from the reaction mixture, thus keeping the majority of the product intact. **BNBN-DBP** was less stable than **BNNB-DBP** due to the presence of one unprotected boron, and thus purification by column chromatography on silica gel or aluminum oxide was unsuccessful, leading to severe hydrolysis. However, **BNBN-DBP** could be purified by careful crystallization from hexane to give a crystalline solid. The solution of **BNBN-DBP** is sensitive to water, so all the characterizations were performed in freshly dried solvents. In contrast, the solid of **BNBN-DBP** is stable and can be stored under ambient conditions, showing no change in the ^{1}H NMR spectra for at least 2 weeks.

Scheme 1. Synthetic Routes to BNNB-DBP and BNBN-DBP.

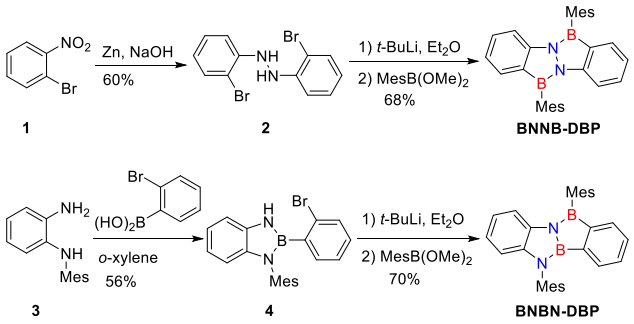

The chemical structures of **BNNB-DBP** and **BNBN-DBP** were fully characterized by ^{1}H, ^{13}C, and ^{11}B NMR spectroscopy as well as high-resolution mass spectrometry. Notably, only one boron signal was observed at 37.3 ppm for **BNNB-DBP**, whereas two signals at 50.4 and 38.3 ppm were recorded for **BNBN-DBP** due to the presence of two kinds of boron atoms. The thermal stability of these two compounds was examined by thermogravimetric analysis (TGA), which revealed high decomposition temperatures of 288 °C for **BNNB-DBP** and 257 °C for **BNBN-DBP** (Figure S1).

BNNB-DBP and **BNBN-DBP** as well as their corresponding precursors were successfully characterized by single crystal X-ray diffraction. The 6-5-5-6 fused ring structures of **BNNB-DBP** and **BNBN-DBP** can be clearly recognized in Figure 1 as fully planar skeletons. The mesityl substituents are almost perpendicular to the conjugated plane with twisting angles of about 70 – 80°. The three bonds connected with the boron atoms (one B−N bond and two B−C bonds) are in the same plane with the sum of the three bond angles of about 360°. As shown in Figure 1d, B and N atoms in **BNBN-DBP** could not be crystallographically distinguished. This phenomenon was caused by the chemically asymmetric BNBN sequence (compared to the centrosymmetric BNNB sequence) in a geometrically centrosymmetric skeleton. The molecules packed in the crystal without any preferred orientation of the embedded BNBN sequence, thus leading to a disordered packing structure. In contrast, **BNNB-DBP** does not have this problem, and provides more detailed structural information. The B−N bond lengths in **BNNB-DBP** are in the range of 1.40 – 1.44 Å, indicative of localized BN double bond character.[19] The N−N bond length is around 1.42 Å, a typical value for N−N single bond (1.40 Å in compound **2**). These structural features indicate that the bond length alteration in **BNNB-DBP** is similar to that in **DBP**.

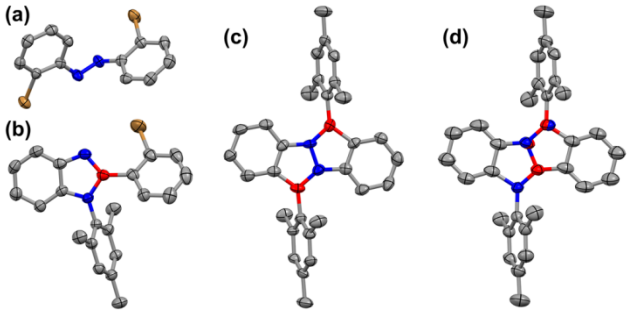

Figure 1. Single-crystal structures of (a) compound **2**, (b) compound **4**, (c) **BNNB-DBP**, and (d) **BNBN-DBP** with thermal ellipsoids shown at 50% probability. Hydrogen atoms are omitted for clarity. B and N atoms in (d) **BNBN-DBP** are not crystallographically distinguishable owing to disorder. Colors: gray, carbon; red, boron; blue, nitrogen; orange, bromine.

To understand how the BN substitution and the orientation patterns of BN units influence the antiaromaticity of **DPB**, we performed nucleus-independent chemical shift (NICS) calculations[20] at the B3LYP/6-311+G(2d,p) level. As illustrated in Figure 2, the parent **DBP** has a highly antiaromatic pentalene core with a large positive NICS(1)$_{zz}$ value of 23.7 ppm and moderately aromatic fused benzene rings. Differently, in **BNNB-DBP**, the fused benzene rings exhibit high aromaticity, whereas the BNNB-substituted pentalene core is almost nonaromatic. In contrast, the asymmetric **BNBN-DBP** has different NICS(1)$_{zz}$ values for each ring. The fused benzene rings are aromatic, with the one on the N side much stronger. Notably, the $BNBC_2$ ring shows a highly antiaromatic feature (18.7 ppm), whereas the $NBNC_2$ ring displays weak aromaticity (–2.6 ppm).

These differences may partly relate to the lone pairs of N atoms and the vacant p orbitals of B atoms. The $BNNC_2$ ring is in principle aromatic with six π-electrons in total (Figure S4). However, when it is incorporated in the fused system of **BNNB-DBP**, the lone pair of N atom is attracted by the extra B atom, which reduces the effective diatropic ring current and leads to lowered aromaticity. Similarly, the (anti)aromatic properties of **BNBN-DBP** can also be rationalized by the presence of six π-electrons in the $NBNC_2$ ring and four π-electrons in the $BNBC_2$ ring. The aromaticity and antiaromaticity are both reduced due to the extra B or N atoms connected to each ring in **BNBN-DBP**. In addition to the effect of the heteroatoms, the global paratropic ring current from these 4*n*π-electron systems further reduces the aromaticity but enhances the antiaromaticity of individual rings.[21] These results indicate that although **DBP** and its BN-embedded derivatives possess the same 4*n*π-electrons in total, the (anti)aromaticity of each ring is significantly modified by the BN substitution, and different BN orientation patterns lead to completely different electronic structures.

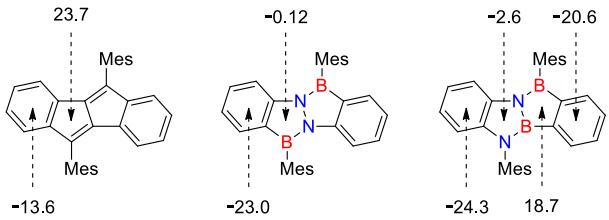

Figure 2. NICS(1)$_{zz}$ values (ppm) of **DBP**, **BNNB-DBP**, and **BNBN-DBP** calculated at the GIAO-B3LYP/6-311+G(2d,p) level.

The photophysical and electrochemical properties of **BNNB-DBP** and **BNBN-DBP** were investigated by UV–Vis absorption

and photoluminescence spectroscopies as well as cyclic voltammetry (CV). As displayed in Figure 3, **BNNB-DBP** displays two main absorption bands peaking at 268 and 342 nm and an absorption onset of 375 nm, which corresponds to an optical bandgap of 3.31 eV. On the other hand, **BNBN-DBP** shows a red-shifted absorption maximum at 279 nm and a very weak absorption between 320 and 400 nm (Figure 3, inset). The optical bandgap deduced from the low-energy absorption onset is 3.10 eV (Figure S3), which is smaller than that of **BNNB-DBP**. Overall, both compounds revealed blue-shifted absorption onsets, that is, larger optical bandgaps, relative to that of **DBP**.[17d] The photoluminescence spectroscopic analysis indicated that the antiaromatic **BNBN-DBP** is non-emissive, which is similar to the case of **DBP**s.[17] In contrast, **BNNB-DBP** featuring a nonaromatic pentalene core exhibited deep blue fluorescence with an emission maximum at 403 nm and a quantum yield of 18%, which is quite unusual in pentalene derivatives. The energy levels of these two compounds were estimated by CV experiments (Figure S2). **BNNB-DBP** possesses a lower HOMO level of −5.93 eV compared to that of **BNBN-DBP** (−5.62 eV), whereas their LUMO levels are quite similar (−2.67 eV for **BNNB-DBP** and −2.60 eV for **BNBN-DBP**). The electrochemical bandgaps of **BNNB-DBP** and **BNBN-DBP** are 3.26 and 3.02 eV, respectively, which agreed well with the optical bandgaps.

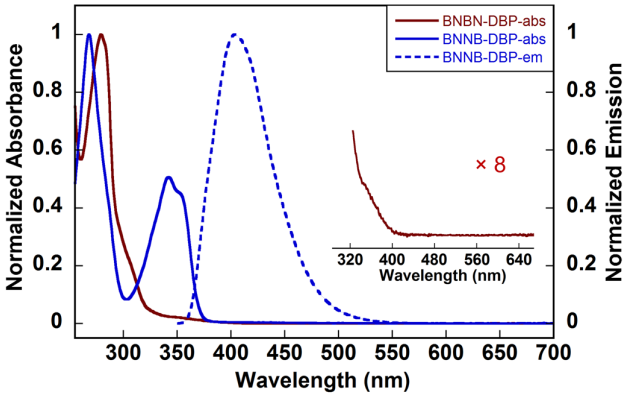

Figure 3. The absorption spectra of **BNNB-DBP** and **BNBN-DBP** as well as the emission spectrum of **BNNB-DBP** (excitation wavelength: 342 nm) in CH_2Cl_2. Inset shows an enlarged region of the absorption spectrum of **BNBN-DBP**.

To gain more insights into the electronic properties of **BNNB-DBP** and **BNBN-DBP** compared to their carbon analogue **DBP**, we performed density functional theory (DFT) calculations at the B3LYP/6-311G(d,p) level. As depicted in Figure 4, BN substitution resulted in completely different electronic structures. First, **BNNB-DBP** and **BNBN-DBP** both exhibited larger bandgaps than the parent **DBP**. **BNBN-DBP** had the same LUMO level as that of **BNNB-DBP**, but a much higher HOMO level and thus a lower bandgap, which is consistent with the experimental results as discussed above. Second, as indicated previously,[17f] the HOMO→LUMO transition of **DBP** is symmetry-forbidden. **BNBN-DBP** maintains the similar character, although the orbital distributions are polarized, with larger HOMO coefficient on the N side and severely localized LUMO on the B side (Figure 4). According to time-dependent DFT (TD-DFT) calculations, the lowest-energy absorption of **BNBN-DBP** can be assigned to the symmetry-forbidden HOMO→LUMO transition, which exhibited an extremely low oscillator strength (*f*) of 0.0001 (Figure S6). In contrast, TD-DFT calculations on **BNNB-DBP** indicated that its HOMO possessed a different symmetry compared to that of **DBP**, while their LUMO symmetries were identical (Figure 4). Therefore, the HOMO→LUMO transition (*f*: 0.2823) of **BNNB-DBP** is allowed, corresponding to the absorption band at 342 nm (Figure 3). These results indicate that different BN substitution patterns lead to significantly distinct electronic structures, which determine their varying photophysical properties.

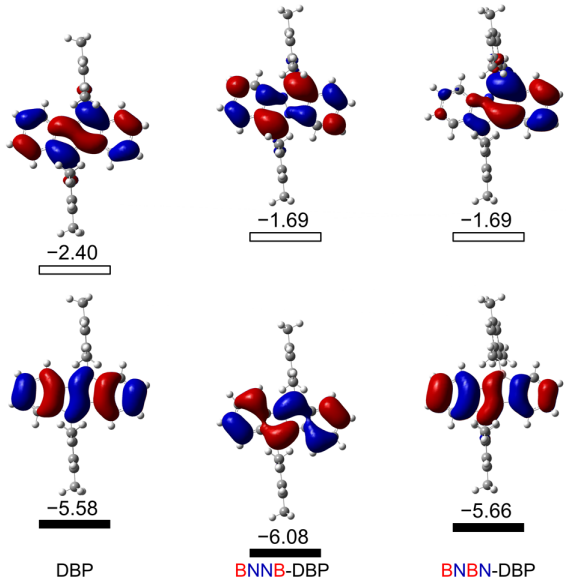

Figure 4. Frontier molecular orbitals and their energy levels (unit: eV) of **DBP**, **BNNB-DBP**, and **BNBN-DBP** calculated at the B3LYP/6-311G(d,p) level.

In summary, two BN-embedded dibenzo[*a,e*]pentalenes, **BNNB-DBP** and **BNBN-DBP** were synthesized through multiple lithiations (on carbon and nitrogen at the same time) followed by nucleophilic substitutions. This strategy can be a promising method for the synthesis of BN-embedded conjugated molecules. Moreover, we have for the first time revealed that different BN orientation patterns significantly influenced the antiaromaticity and the optical and electronic properties. These results indicate that precise control of the BN orientation pattern is of great importance to effectively modulate the chemical and physical properties of conjugated molecules embedded with more than one BN unit. Further exploration of the BN substitution strategy in antiaromatic systems can open up new possibilities to extend the scope of antiaromatic molecules and deepen the fundamental understanding of antiaromaticity.

ASSOCIATED CONTENT

Supporting Information

Experimental details, synthesis, characterizations, single crystal data (CIF), computational studies, and NMR spectra. This material is available free of charge via the Internet at http://pubs.acs.org."

AUTHOR INFORMATION

Corresponding Author

xinliang.feng@tu-dresden.de
muellen@mpip-mainz.mpg.de

Notes

The authors declare no competing financial interests.

ACKNOWLEDGMENT

The authors sincerely thank Wen Zhang for high-resolution MALDI-TOF MS measurements and Dr. Dieter Schollmeyer (Institute for Organic Chemistry, Johannes Gutenberg University Mainz) for single-crystal X-ray structural analysis. We are grate-

ful for the financial support from the European Research Council grant on NANOGRAPH, DFG Priority Program SPP 1459, Graphene Flagship (No. CNECT-ICT-604391), and European Union Projects UPGRADE and MoQuaS.

REFERENCES

(1) Minkin, V. I.; Glukhovtsev, M. N.; Simkin, B. Y. *Aromaticity and Antiaromaticity: Electronic and Structural Aspects*; John Wiely & Sons: New York, 1994.

(2) For reviews, see: (a) Wang, X.-Y.; Wang, J.-Y.; Pei, J. *Chem. Eur. J.* **2015**, *21*, 3528. (b) Campbell, P. G.; Marwitz, A. J. V.; Liu, S. Y. *Angew. Chem. Int. Ed.* **2012**, *51*, 6074. (c) Bosdet, M. J. D.; Piers, W. E. *Can. J. Chem.* **2009**, *87*, 8. (d) Liu, Z. Q.; Marder, T. B. *Angew. Chem. Int. Ed.* **2008**, *47*, 242.

(3) (a) Xu, S.; Mikulas, T. C.; Zakharov, L. N.; Dixon, D. A.; Liu, S.-Y. *Angew. Chem. Int. Ed.* **2013**, *52*, 7527. (b) Campbell, P. G.; Abbey, E. R.; Neiner, D.; Grant, D. J.; Dixon, D. A.; Liu, S.-Y. *J. Am. Chem. Soc.* **2010**, *132*, 18048. (c) Abbey, E. R.; Zakharov, L. N.; Liu, S.-Y. *J. Am. Chem. Soc.* **2008**, *130*, 7250.

(4) Campbell, P. G.; Zakharov, L. N.; Grant, D. J.; Dixon, D. A.; Liu, S.-Y. *J. Am. Chem. Soc.* **2010**, *132*, 3289.

(5) Knack, D. H.; Marshall, J. L.; Harlow, G. P.; Dudzik, A.; Szaleniec, M.; Liu, S.-Y.; Heider, J. *Angew. Chem. Int. Ed.* **2013**, *52*, 2599.

(6) (a) Wang, X.-Y.; Lin, H.-R.; Lei, T.; Yang, D.-C.; Zhuang, F.-D.; Wang, J.-Y.; Yuan, S.-C.; Pei, J. *Angew. Chem. Int. Ed.* **2013**, *52*, 3117. (b) Wang, X.-Y.; Zhuang, F.-D.; Zhou, X.; Yang, D.-C.; Wang, J.-Y.; Pei, J. *J. Mater. Chem. C* **2014**, *2*, 8152. (c) Wang, X.-Y.; Zhuang, F.-D.; Wang, R.-B.; Wang, X.-C.; Cao, X.-Y.; Wang, J.-Y.; Pei, J. *J. Am. Chem. Soc.* **2014**, *136*, 3764. (d) Wang, X.; Zhang, F.; Liu, J.; Tang, R. Z.; Fu, Y. B.; Wu, D. Q.; Xu, Q.; Zhuang, X. D.; He, G. F.; Feng, X. L. *Org. Lett.* **2013**, *15*, 5714. (e) Hashimoto, S.; Ikuta, T.; Shiren, K.; Nakatsuka, S.; Ni, J.; Nakamura, M.; Hatakeyama, T. *Chem. Mater.* **2014**, *26*, 6265. (f) Li, G.; Zhao, Y.; Li, J.; Cao, J.; Zhu, J.; Sun, X. W.; Zhang, Q. *J. Org. Chem.* **2015**, *80*, 196.

(7) (a) Baggett, A. W.; Vasiliu, M.; Li, B.; Dixon, D. A.; Liu, S.-Y. *J. Am. Chem. Soc.* **2015**, *137*, 5536. (b) Abbey, E. R.; Lamm, A. N.; Baggett, A. W.; Zakharov, L. N.; Liu, S.-Y. *J. Am. Chem. Soc.* **2013**, *135*, 12908. (c) Braunschweig, H.; Geetharani, K.; Jimenez-Halla, J. O. C.; Schäfer, M. *Angew. Chem. Int. Ed.* **2014**, *53*, 3500. (d) Ashe III, A. J.; Fang, X. D. *Org. Lett.* **2000**, *2*, 2089.

(8) (a) Liu, X.; Wu, P.; Li, J.; Cui, C. *J. Org. Chem.* **2015**, *80*, 3737. (b) Wisniewski, S. R.; Guenther, C. L.; Argintaru, O. A.; Molander, G. A. *J. Org. Chem.* **2014**, *79*, 365. (c) Fang, X. D.; Yang, H.; Kampf, J. W.; Holl, M. M. B.; Ashe III, A. J. *Organometallics* **2006**, *25*, 513.

(9) (a) Chrostowska, A.; Xu, S.; Mazière, A.; Boknevitz, K.; Li, B.; Abbey, E. R.; Dargelos, A.; Graciaa, A.; Liu, S.-Y. *J. Am. Chem. Soc.* **2014**, *136*, 11813. (b) Abbey, E. R.; Zakharov, L. N.; Liu, S.-Y. *J. Am. Chem. Soc.* **2011**, *133*, 11508.

(10) (a) Bosdet, M. J. D.; Jaska, C. A.; Piers, W. E.; Sorensen, T. S.; Parvez, M. *Org. Lett.* **2007**, *9*, 1395. (b) Lu, J. S.; Ko, S. B.; Walters, N. R.; Kang, Y.; Sauriol, F.; Wang, S. N. *Angew. Chem. Int. Ed.* **2013**, *52*, 4544.

(11) Ishibashi, J. S. A.; Marshall, J. L.; Mazière, A.; Lovinger, G. J.; Li, B.; Zakharov, L. N.; Dargelos, A.; Graciaa, A.; Chrostowska, A.; Liu, S.-Y. *J. Am. Chem. Soc.* **2014**, *136*, 15414.

(12) Jaska, C. A.; Emslie, D. J. H.; Bosdet, M. J. D.; Piers, W. E.; Sorensen, T. S.; Parvez, M. *J. Am. Chem. Soc.* **2006**, *128*, 10885.

(13) Bosdet, M. J. D.; Piers, W. E.; Sorensen, T. S.; Parvez, M. *Angew. Chem. Int. Ed.* **2007**, *46*, 4940.

(14) (a) Wang, X.-Y.; Zhuang, F.-D.; Wang, X.-C.; Cao, X.-Y.; Wang, J.-Y.; Pei, J. *Chem. Commun.* **2015**, *51*, 4368. (b) Li, G.; Xiong, W.-W.; Gu, P.-Y.; Cao, J.; Zhu, J.; Ganguly, R.; Li, Y.; Grimsdale, A. C.; Zhang, Q. *Org. Lett.* **2015**, *17*, 560.

(15) (a) Neue, B.; Araneda, J. F.; Piers, W. E.; Parvez, M. *Angew. Chem. Int. Ed.* **2013**, *52*, 9966. (b) Müller, M.; Behnle, S.; Maichle-Mossmer, C.; Bettinger, H. F. *Chem. Commun.* **2014**, *50*, 7821. (c) Hatakeyama, T.; Hashimoto, S.; Seki, S.; Nakamura, M. *J. Am. Chem. Soc.* **2011**, *133*, 18614. (d) Lepeltier, M.; Lukoyanova, O.; Jacobson, A.; Jeeva, S.; Perepichka, D. F. *Chem. Commun.* **2010**, *46*, 7007.

(16) For reviews, see: (a) Hopf, H. *Angew. Chem. Int. Ed.* **2013**, *52*, 12224. (b) Saito, M. *Symmetry* **2010**, *2*, 950.

(17) (a) Li, H.; Wang, X.-Y.; Wei, B.; Xu, L.; Zhang, W.-X.; Pei, J.; Xi, Z. *Nat. Commun.* **2014**, *5*, 4508. (b) Zhao, J.; Oniwa, K.; Asao, N.; Yamamoto, Y.; Jin, T. *J. Am. Chem. Soc.* **2013**, *135*, 10222. (c) Chen, C.; Harhausen, M.; Liedtke, R.; Bussmann, K.; Fukazawa, A.; Yamaguchi, S.; Petersen, J. L.; Daniliuc, C. G.; Fröhlich, R.; Kehr, G.; Erker, G. *Angew. Chem. Int. Ed.* **2013**, *52*, 5992. (d) Maekawa, T.; Segawa, Y.; Itami, K. *Chem. Sci.* **2013**, *4*, 2369. (e) Levi, Z. U.; Tilley, T. D. *J. Am. Chem. Soc.* **2009**, *131*, 2796. (f) Kawase, T.; Fujiwara, T.; Kitamura, C.; Konishi, A.; Hirao, Y.; Matsumoto, K.; Kurata, H.; Kubo, T.; Shinamura, S.; Mori, H.; Miyazaki, E.; Takimiya, K. *Angew. Chem. Int. Ed.* **2010**, *49*, 7728.

(18) During the preparation of this manuscript, Cui *et al*. reported an elegant synthesis of BNNB-substituted benzopentalenes by electrophilic borylation from hydrazones. See: Ma, C.; Zhang, J.; Li, J.; Cui, C. *Chem. Commun.* **2015**, *51*, 5732.

(19) Abbey, E. R.; Zakharov, L. N.; Liu, S. Y. *J. Am. Chem. Soc.* **2008**, *130*, 7250.

(20) Chen, Z.; Wannere, C. S.; Corminboeuf, C.; Puchta, R.; Schleyer, P. v. R. *Chem. Rev.* **2005**, *105*, 3842.

(21) Cao, J.; London, G.; Dumele, O.; von Wantoch Rekowski, M.; Trapp, N.; Ruhlmann, L.; Boudon, C.; Stanger, A.; Diederich, F. *J. Am. Chem. Soc.* **2015,** DOI: 10.1021/jacs.5b03074.

Table of Contents Graphic